Journal of Solid State Chemistry 182 (2009) 1786–1791

Contents lists available at ScienceDirect

Journal of Solid State Chemistry

journal homepage: www.elsevier.com/locate/jssc

The phase transition of the incommensurate phases β-$Ln(PO_3)_3$ ($Ln = Y, Tb \ldots Yb$), crystal structures of α-$Ln(PO_3)_3$ ($Ln = Y, Tb \ldots Yb$) and $Sc(PO_3)_3$

Hennig A. Höppe *

Institut für Anorganische und Analytische Chemie, Albert-Ludwigs-Universität Freiburg, Albertstr. 21, D-79104 Freiburg, Germany

ARTICLE INFO

Article history:
Received 7 December 2008
Received in revised form
20 February 2009
Accepted 25 February 2009
Available online 18 April 2009

Keywords:
Crystal structure
Lanthanide
Phosphate
Phase transition
Vibrational spectroscopy

ABSTRACT

The incommensurately modulated room-temperature phases β-$Ln(PO_3)_3$ ($Ln = Y, Tb \ldots Yb$) undergo a topotactic phase transition monitored by vibrational spectroscopy below 180 K leading to α-$Ln(PO_3)_3$ ($Ln = Y, Dy \ldots Yb$), above 200 K the incommensurate phases are reobtained. The low-temperature phases exhibit a new structure type (α-$Dy(PO_3)_3$, $P2_1/c$, $Z = 12, a = 14.1422(6)$, $b = 20.0793(9), c = 10.1018(4)$ Å, $\beta = 127.532(3)^\circ$). α-$Tb(PO_3)_3$ is isotypic with $Gd(PO_3)_3$ (α-$Tb(PO_3)_3$, $I2/a, Z = 16, a = 25.875(6)$, $b = 13.460(3)$, $c = 10.044(2)$ Å, $\beta = 119.13(3)^\circ$). The symmetry relations between the involved phases of the phase transition are discussed. The crystal structure of $Sc(PO_3)_3$ is isotypic with that of $Lu(PO_3)_3$ and *C*-type phosphates. The polyphosphates consist of infinite zig-zag chains of corner-sharing PO_4 tetrahedra, the cations are coordinated sixfold in an almost octahedral arrangement. To confirm the quality of the determined crystal structures the deviation of the phosphate tetrahedra from ideal symmetry was determined and discussed.

1. Introduction

Crystalline compounds of rare-earth metals with condensed anions are of broad interest for optical applications [1,2], but unfortunately there are still some inconsistencies of structural parameters in many condensed phosphates containing heavily distorted PO_4 units in which the phosphorus atom is occasionally almost outside the tetrahedron [3,4] which have unfortunately found their way into respective monographs [5]. Therefore it is our approach to clarify the coordination environment around the lanthanoid ions by a careful determination of their crystal structures and then to identify suitable host lattices useful for optical applications, like e.g. quantum cutting phosphors [6] or as upconversion phosphors in solar cells [7]. When we reported on the crystal structures of the late lanthanoids' polyphosphate crystal structure [8], we did not report about the Yttrium and Scandium compound. Recently, Murashova et al. published an approximant of the incommensurate $Er(PO_3)_3$ [8] as an 11-fold superstructure [9] of the basic unit cell.

The previously mentioned unacceptably high distortion of the phosphate tetrahedra from the ideal symmetry normally found in *catena*-phosphates like α-$Sr(PO_3)_3$ [10] or Trömelite [11] will be determined and compared with the crystal structure elucidations presented in [8,3] and this contribution. The deviation from ideal symmetry was calculated applying the method of all ligands enclosing spheres [12,13] on experimental data.

For practical reasons I will refer to the incommensurate phases as β-phases and the low-temperature lock-in phases I will call α-phases.

2. Experimental section

2.1. Synthesis

The synthesis of the title compounds starting from lanthanide oxide and diammonium hydrogenphosphate was performed according to

$$Ln_2O_3 + 6(NH_4)_2HPO_4 \rightarrow 2Ln(PO_3)_3 + 12NH_3 + 9H_2O \quad (1)$$

for $Ln = Sc, Y, Tb \ldots Yb$. The synthesis process is described on the yttrium compound, the others are obtained analogously.

The carefully ground mixture of 57.0 mg (0.252 mmol) yttrium oxide (Kristallhandel Kelpin, 99.9%) and 217.9 mg (1.650 mmol) ammonium dihydrogenphosphate (ABCR, 98%) was transferred into an alumina crucible. The latter was then heated to 873 K with a rate of 120 K h^{-1} and maintained at this temperature for 8 h. After cooling to room temperature with a rate of 60 K h^{-1} 161 mg (0.494 mmol, 98%) $Y(PO_3)_3$ were obtained as a crystalline, colourless and non-hygroscopic powder.

* Fax: +49 7612036012.
E-mail address: henning.hoeppe@ac.uni-freiburg.de

0022-4596/$ - see front matter © 2009 Elsevier Inc. All rights reserved.
doi:10.1016/j.jssc.2009.02.036

The composition of the obtained samples was checked by energy dispersive X-ray spectroscopy (EDX) and confirmed the respective *Ln* : P ratios.

2.2. Vibrational spectroscopy

Temperature-dependent FTIR spectra were obtained at room temperature by using a Bruker IFS 66v/S spectrometer. The samples were thoroughly mixed with dried KBr (approx. 2 mg sample, 300 mg KBr) and then pressed to transparent pellets. The temperature was allowed to stabilise for 10 min every 10° before the spectrum was recorded.

Table 1
Crystallographic data for β-$Y(PO_3)_3$ and $Sc(PO_3)_3$ with esds in parentheses.

Formula	β-$Y(PO_3)_3$	$Sc(PO_3)_3$
Temperature		293 K
Space group, Z	$Cc(0\beta0)0$, 4 $\beta = 0.364(1)$	Cc, 12
Cell parameters	$a = 14.125(2)$ Å	$a = 13.5459(5)$ Å
	$b = 6.6931(6)$ Å	$b = 19.5147(9)$ Å
	$\beta = 127.557(8)°$	$\beta = 127.172(3)°$
	$c = 10.0453(12)$ Å	$c = 9.6796(5)$ Å
X-ray density ($g\,cm^{-3}$)	2.874	2.760
$F(000)$	624	1656
Abs. coeff. μ (mm^{-1})	8.41	1.82
Diffractometer	Stoe IPDS II	Bruker AXS CCD (APEX-II)
Radiation		$\lambda = 0.71073$ Å (Mo$K\alpha$)
Crystal size (mm^3)	$0.06 \times 0.05 \times 0.04$	$0.04 \times 0.03 \times 0.03$
Max. diffract. angle (°)	50.0	50.0
$h_{max}/k_{max}/l_{max}/m_{max}$	21/10/14/1	15/23/11
Observed/unique reflections	2675/8238	1984/3510
R_{int}/R_σ	0.158/0.122	0.134/0.110
Corrections		Lorentz, polarisation, extinction, absorption
Refined parameters	195	252
Extinction coefficient	0.004(1)	0.00013(5)
Flack parameter	0.49(1)	0.51(1)
GoF	1.98	0.919
R indices (all data)	$R_{all} = 0.067$, $wR_{all} = 0.140$, $R_{sat} = 0.097$, $wR_{sat} = 0.188$	$R1 = 0.049$, $wR2 = 0.094$

2.3. Crystal structure determinations

X-ray diffraction data were collected on a Stoe IPDS II area detection diffractometer at room temperature and on a Bruker AXS CCD (APEX-II) diffractometer at 100 K. Further details of the crystal structure investigations (especially the coefficients of the modulation functions) may be obtained from the Fachinformationszentrum Karlsruhe, D-76344 Eggenstein-Leopoldshafen, Germany (e-mail: crysdata@fiz-karlsruhe.de) on quoting the depository numbers CSD-420120 ($Sc(PO_3)_3$), CSD-420121 (β-$Y(PO_3)_3$), CSD-420122 (α-$Y(PO_3)_3$), CSD-420118 (α-$Tb(PO_3)_3$), CSD-420123 (α-$Dy(PO_3)_3$), CSD-420117 (α-$Ho(PO_3)_3$), CSD-420116 (α-$Er(PO_3)_3$) and CSD-420119 (α-$Tm(PO_3)_3$) the name of the author and citation of this publication.

2.3.1. β-$Y(PO_3)_3$ at room temperature

The basic diffraction pattern was indexed on the basis of a *C*-centred monoclinic unit cell. According to the diffraction pattern satellite reflections besides the normal Bragg reflections were found which could be indexed considering an incommensurate modulation vector $\boldsymbol{q} \approx 0.36\mathbf{b}^*$. The crystal structure of $Y(PO_3)_3$ was solved by direct methods using SHELXS [14] and refined with anisotropic displacement parameters and positional modulation waves for all atoms using the JANA2006 package [15]. The parameters of the room-temperature single-crystal data collection and the refinement of β-$Y(PO_3)_3$ are given in Table 1. The positional and displacement parameters as well as the modulation function parameters for all atoms are given in the CIF. The obtained crystalline products were phase pure according to X-ray powder diffractometry.

2.3.2. Crystal structures of the lock-in phases α-$Ln(PO_3)_3$ at 100 K

Cooling of single-crystals of the incommensurate β-phases led to topotactic phase transitions to form commensurate lock-in α-phases.

The diffraction patterns were indexed on the basis of a primitive monoclinic unit cell. The crystal structures of α-$Ln(PO_3)_3$ ($Ln = Dy, Ho, Er, Tm, Y$) were solved in space group $P2_1/c$ by direct methods using SHELXTL [14] and refined with anisotropic displacement parameters for all atoms. The parameters of the single-crystal data collections and the refinements of α-$Ln(PO_3)_3$ ($Ln = Dy, Ho, Er, Tm, Y$) are given in Table 2. The crystals of α-$Tm(PO_3)_3$ and α-$Y(PO_3)_3$ showed some

Table 2
Crystallographic data and parameters of the structure refinements for α-$Ln(PO_3)_3$ (Ln = Tb, Dy, Ho, Er, Tm, Y) with esds in parentheses.

α-$Ln(PO_3)_3$ Temperature	Tb 100 K	Dy	Ho	Er	Tm	Y
Space group, Z	$I2/a$, 16	$P2_1/c$, 12	$P2_1/c$, 12	$P2_1/c$, 12	$P2_1/c$, 12	$P2_1/c$, 12
a (Å)	25.875(6)	14.1422(6)	14.1097(3)	14.0630(5)	14.0447(12)	14.1062(6)
b (Å)	13.460(3)	20.0793(9)	20.0278(4)	19.9811(7)	19.917(2)	20.0282(9)
β (°)	119.13(3)	127.532(3)	127.508(1)	127.600(2)	127.566(6)	127.48(2)
c (Å)	10.044(2)	10.1018(4)	10.0830(2)	10.0357(3)	10.0365(8)	10.0802(4)
X-ray density ($g\,cm^{-3}$)	3.442	3.499	3.543	3.605	3.634	2.873
$F(000)$	2912	2196	2208	2220	2232	1872
Abs. coeff. μ (mm^{-1})	9.91	10.51	11.16	11.94	12.63	8.40
Diffractometer	Bruker AXS CCD (APEX-II), $\lambda = 0.71073$ Å (Mo$K\alpha$)					
Max. diffract. angle (°)	40.0	50.0	50.0	50.0	50.0	50.0
$h_{max}/k_{max}/l_{max}$	24/12/9	16/23/12	15/18/11	16/23/11	16/23/11	16/23/11
Observed/unique reflections	1029/1387	2828/3984	2486/3882	2542/3923	2441/3884	2094/3957
R_{int}/R_σ	0.137/0.173	0.067/0.044	0.080/0.071	0.090/0.037	0.136/0.074	0.213/0.125
Corrections	Lorentz, polarisation, Extinction, absorption					
Refined parameters	237	355	308	349	332	332
Extinction coefficient	0.0014(2)	0	0.00004(1)	0	0.00071(6)	0.00032(6)
GoF	1.083	0.969	0.899	1.009	1.009	0.883
$R1$, $wR2$ (all data)	0.097/0.155	0.036/0.081	0.037/0.063	0.034/0.076	0.043/0.093	0.053/0.104

polycrystalline fractions already while initial images of single-crystals of α-$Yb(PO_3)_3$ could only be indexed at low temperature before they turned into polycrystalline samples. But the gained information was sufficient to prove the isotypicity with α-$Dy(PO_3)_3$.

The diffraction pattern of α-$Tb(PO_3)_3$ was indexed on the basis of a *C*-centered monoclinic unit cell. The crystal structure was solved in space group *I*2/*a* by direct methods using SHELXTL [14] and refined with anisotropic displacement parameters for all atoms. The parameters of the single-crystal data collection and the refinement of α-$Tb(PO_3)_3$ are given in Table 2.

2.3.3. $Sc(PO_3)_3$

The diffraction pattern was indexed on the basis of a *C*-centred monoclinic unit cell. The crystal structure of $Sc(PO_3)_3$ was solved in space group *Cc* (no. 9) by direct methods using SHELXTL [14] and refined with anisotropic displacement parameters for all atoms. The data set has been corrected for absorption by applying a numerical correction based on an optimised crystal shape by the program X-Shape (Stoe & Cie., Darmstadt, Germany). The parameters of the room-temperature single-crystal data collection and the refinement of $Sc(PO_3)_3$ are given in Table 1, the positional and displacement parameters for all atoms are given in the CIF.

3. Phase transition monitored by vibrational spectroscopy

The most obvious effect of the modulation on the crystal structure is the displacement of the heavy atoms and a very strong distortion of the polyphosphate chain [8]. Therefore I decided to follow the phase transition by *in situ* IR spectroscopy which was found to be best in the region of the P–O–P vibrations between 600 and 800 cm^{-1}. The temperature dependent measurements show clearly an evolution of two vibrational bands by cooling below 180 K and the reverse effect by heating above 200 K as displayed in Fig. 1. Obviously, the phase transition shows a hysteresis typical for a first order phase transition. Like the modulation vector the phase transition temperatures of all investigated samples are very similar to those observed for $Tb(PO_3)_3$. Since all spectra are very similar only the measurements of $Tb(PO_3)_3$ are displayed. The phase transition is very hard to observe by DSC measurements because the caloric effect is very weak (approx. 0.3 kJ mol^{-1}).

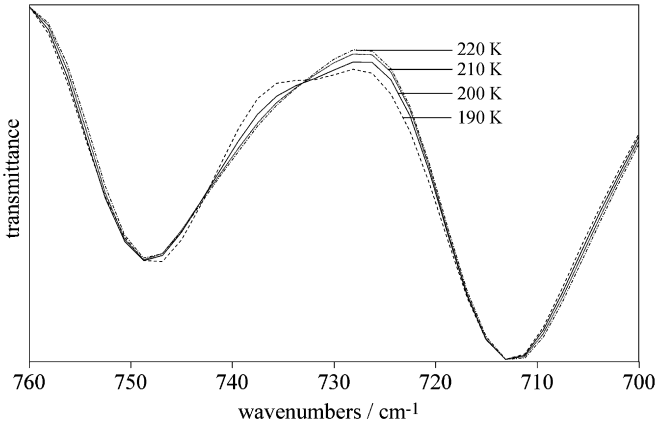

Fig. 1. Temperature dependent IR spectra of $Tb(PO_3)_3$; heating above 200 K leads to the incommensurate β-phases, cooling below 180 K gives the α-phases.

4. Crystal structures

The crystal structures consist of infinite zig-zag chains of PO_4 tetrahedra connected by common corners giving the polyphosphate anion PO_3^-. In-between these chains in the basic unit cell (Fig. 2) the lanthanoid cations are positioned and coordinated by six terminal oxygen atoms forming slightly distorted octahedra.

4.1. Incommensurately modulated β-$Y(PO_3)_3$ at room temperature

Considering the satellite reflections which obey the modulation vector $q = 0.364(1)\mathbf{b}^*$ positional sinoidal modulation waves were initially introduced for the Y atoms. The polyphosphate chains apparently respond to this modulation and therefore analogous modulation waves were introduced applying soft restraints on bond lengths inside the phosphate chain. As a result finally almost constant P–O distances (138–154 pm) and angles (96−123°) over the whole modulation period were obtained. The Y atoms are coordinated by terminal oxygen atoms only. Also, the Y–O distances (218–222 pm) and angles O–Y–O (approx. 90° and 180°) vary in a rather close range giving an almost octahedral coordination sphere at every point of the modulation period. Consequently, the anharmonic displacement parameters adopt reasonable values and give quite spherical ellipsoids for all atoms.

4.2. The lock-in phases α-$Ln(PO_3)_3$ (*Ln* = *Tb* … *Yb*, *Y*) at 100 K

α-$Ln(PO_3)_3$ (*Ln* = Dy, Ho, Er, Tm, Yb, Y) crystallise in a new structure type in space group $P2_1/c$ which can be understood as a threefold superstructure along [010] of the above described basic unit cell (Fig. 3). In $Ln(PO_3)_3$ the four crystallographically different *Ln* atoms are coordinated sixfold in an almost octahedral arrangement, two of them located on an inversion centre, with typical *Ln*−O distances displayed in Table 3. The distances between bridging oxygen atoms and P lie between 155 and 162 pm, and for terminal oxygen atoms distances in the range from 144 to 150 pm to adjacent P atoms are found. All these bond lengths are in accordance with the sum of ionic radii of the respective ions [16]. The positional and displacement parameters for all atoms are given in the respective CIF.

The lock-in phases α-$Ln(PO_3)_3$ (*Ln* = Dy, Ho, Er, Tm, Yb, Y) lost the *C*-centring of the incommensurately modulated phases. This structural detail can best be recognised by looking at the phosphate chains in Fig. 3. After the phase transformation these are slightly distorted from the very symmetric habit as observed for the modulated basic cell and consequently the *C*-centring is

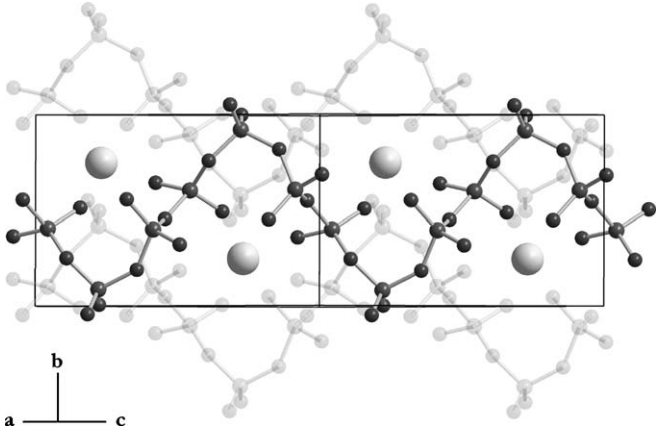

Fig. 2. Basic unit cell of $Ln(PO_3)_3$ (*Ln* = Gd … Lu, Y, Sc).

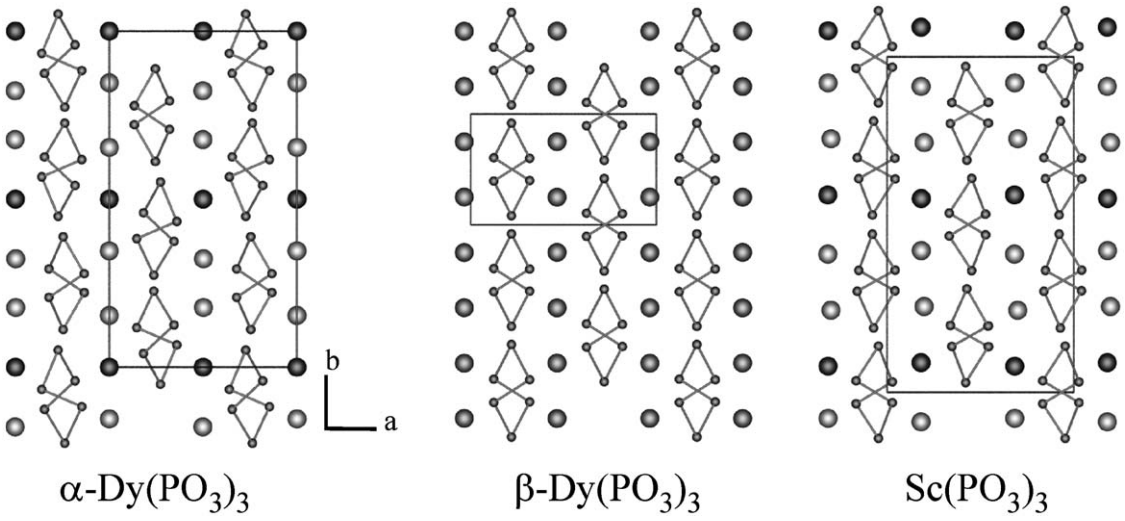

Fig. 3. Comparison of the crystal structures of α-$Dy(PO_3)_3$ (left), incommensurately modulated β-$Dy(PO_3)_3$ (middle) and $Sc(PO_3)_3$ (right); the oxygen atoms have been omitted for clarity and the phosphorus atoms have been connected by fictitious lines to visualise the connectivity of the tetrahedron centres.

Table 3
Selected interatomic distances/pm and angles/° in α-$Ln(PO_3)_3$ (Ln = Dy, Ho, Er, Tm, Y) with esds in parentheses.

α-$(PO_3)_3$	Dy	Ho	Er	Tm	Y
*Ln*1−O	224.4(7)–228.9(7)	222.3(7)–227.5(8)	218.4(8)–224.3(9)	221.2(10)–224.9(10)	222.1(7)–228.7(7)
*Ln*2−O	222.4(7)–226.1(7)	221.4(7)–226.0(8)	218.5(9)–222.3(8)	219.2(9)–224.1(9)	220.6(7)–224.6(6)
*Ln*3−O	225.0(7)–226.6(7)	223.4(8)–225.3(7)	219.7(9)–223.9(8)	220.0(10)–224.6(9)	222.3(8)–225.6(7)
*Ln*4−O	223.2(7)–224.3(7)	221.7(8)–225.6(8)	217.6(8)–221.4(9)	219.8(10)–222.6(10)	222.0(7)–224.8(7)
$P-O^{br}$	158.3(8)–160.0(7)	157.1(8)–160.8(8)	156.2(9)–162.7(8)	157.4(9)–160.5(10)	157.5(8)–160.7(7)
$P-O^{term}$	147.7(8)–149.0(7)	146.4(8)–149.6(8)	144.5(9)–149.5(9)	146.4(11)–150.5(11)	146.8(8)–149.8(8)
P–O–P	133.0(5)–144.2(5)	133.4(5)–144.7(6)	132.1(6)–143.0(6)	131.5(7)–144.2(7)	132.7(5)–144.9(6)

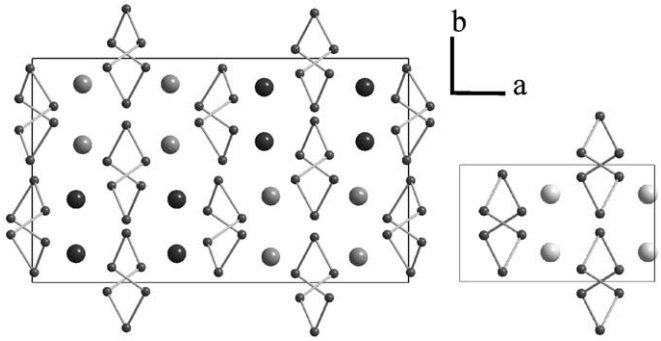

Fig. 4. Comparison of the crystal structures of α-$Tb(PO_3)_3$ (left) and the basic unit cell of the modulated phases β-$Ln(PO_3)_3$ (Ln = Y, Tb … Yb) (right); the oxygen atoms have been omitted for clarity and the phosphorus atoms have been connected by fictitious lines to visualise the connectivity of the tetrahedron centres.

lost. In contrast to the phosphate chains the heavy atoms maintain the *C*-centring.

α-$Tb(PO_3)_3$ crystallises isotypically with $Gd(PO_3)_3$ [8] in space group $I2/a$. Its unit cell represents a fourfold superstructure of the basic unit cell generating an inversion centre which can be understood in terms of chemical twinning [17,18]. To clarify the relationship between the basic structure unit cell of the incommensurate phases and the crystal structure of α-$Tb(PO_3)_3$ the unconventional setting of space group $C2/c$ was chosen (Fig. 4). The terbium atoms are coordinated almost octahedrally with distances between 223 and 233 pm. The distances between bridging oxygen atoms and P lie between 157 and 161 pm, and for terminal oxygen atoms distances in the range from 147 and 150 pm to adjacent P atoms are found. All these bond lengths are in accordance with the sum of ionic radii of the respective ions [16].

The relevant crystallographic data and further details of the X-ray data collections are summarised in Table 2. In Table 3 selected interatomic distances and angles are listed and Table 4 contains the atomic coordinates of α-$Dy(PO_3)_3$ as representative of the new structure type.

4.3. Symmetry relations between α-$Ln(PO_3)_3$ and β-$Ln(PO_3)_3$ (Ln = Tb … Tm, Y)

The phase transition between the incommensurate β- and the lock-in α-phase is apparently topotactic, otherwise an observation on the same single-crystal would be impossible. Therefore there have to exist close crystallographic relationships between both phases. Fig. 5 represents the respective group–subgroup relations. The phase transition occurs via the common super-group $C2/c$ of the respective space-groups. The observed ordering processes do not require large movements of the atoms but they nevertheless lead to tensions in the crystals as mentioned before.

Table 4

Atomic coordinates and isotropic displacement parameters $U_{eq}/Å^2$ for α-$Dy(PO_3)_3$ with esds in parentheses.

Atom	Wyckoff s.	x	y	z	U_{eq}
Dy1	4e	0.50169(4)	0.32250(2)	0.52994(5)	0.02321(12)
Dy2	4e	0.00018(4)	0.84612(2)	−0.51872(5)	0.02312(12)
Dy3	2d	½	½	0	0.02269(14)
Dy4	2a	0	0	0	0.02324(14)
P1	4e	0.2728(2)	0.94906(12)	−0.2606(3)	0.0241(5)
O11	4e	0.3887(6)	0.9133(4)	−0.1671(8)	0.0328(15)
O12	4e	0.1620(6)	0.9104(3)	−0.3753(8)	0.0298(14)
P2	4e	−0.1823(2)	0.95928(12)	−0.8636(3)	0.0246(5)
O21	4e	−0.1221(6)	0.9870(3)	−0.9317(8)	0.0297(14)
O22	4e	−0.1084(7)	0.9300(4)	−0.6942(8)	0.0325(15)
P3	4e	0.3452(2)	0.12551(12)	0.1687(3)	0.0247(5)
O31	4e	0.3779(6)	0.0749(4)	0.2969(8)	0.0293(15)
O32	4e	0.4412(6)	0.1666(3)	0.1925(8)	0.0304(14)
P4	4e	0.2374(2)	0.22629(11)	0.2462(3)	0.0245(5)
O41	4e	0.3604(6)	0.2404(3)	0.3992(7)	0.0287(14)
O42	4e	0.1655(6)	0.2845(3)	0.1409(8)	0.0308(14)
P5	4e	0.1463(2)	0.38244(12)	−0.1619(3)	0.0237(5)
O51	4e	0.1272(6)	0.4324(4)	−0.2852(8)	0.0297(15)
O52	4e	0.0552(6)	0.3801(3)	−0.1343(8)	0.0288(14)
P6	4e	0.3600(2)	0.43368(12)	0.1695(3)	0.0232(5)
O61	4e	0.3910(6)	0.3959(4)	0.3157(8)	0.0308(15)
O62	4e	0.4578(6)	0.4588(3)	0.1666(8)	0.0274(14)
O1	4e	−0.2683(6)	0.0148(3)	−0.8756(7)	0.0262(14)
O2	4e	−0.2785(6)	0.9056(4)	−0.9877(8)	0.0335(15)
O3	4e	0.2416(6)	0.1722(3)	0.1339(8)	0.0263(14)
O4	4e	0.1583(6)	0.3093(3)	−0.2116(8)	0.0257(13)
O5	4e	0.2763(6)	0.3893(3)	0.0073(8)	0.0321(15)
O6	4e	0.2698(6)	0.0078(3)	−0.3702(7)	0.0255(13)
P7	4e	0.6786(2)	0.29225(12)	0.3766(3)	0.0242(5)
O71	4e	0.6004(6)	0.3076(3)	0.4225(8)	0.0316(15)
O72	4e	0.6391(7)	0.2433(4)	0.2422(9)	0.0327(15)
P8	4e	0.1334(2)	0.72182(12)	−0.1917(3)	0.0242(5)
O81	4e	0.0948(6)	0.7586(4)	−0.3444(8)	0.0308(15)
O82	4e	0.0414(6)	0.6847(3)	−0.1929(8)	0.0288(13)
P9	4e	0.2458(2)	0.61191(12)	−0.2308(3)	0.0244(5)
O91	4e	0.3425(6)	0.5674(3)	−0.1018(8)	0.0295(14)
O92	4e	0.1222(6)	0.5852(3)	−0.3484(8)	0.0304(14)
O7	4e	0.8058(6)	0.2722(4)	0.5398(8)	0.0327(15)
O8	4e	0.2431(6)	0.6744(3)	−0.1359(8)	0.0258(13)
O9	4e	0.7140(7)	0.3597(3)	0.3369(8)	0.0295(15)

U_{eq} is defined as one third of the trace of the U_{ij} tensor.

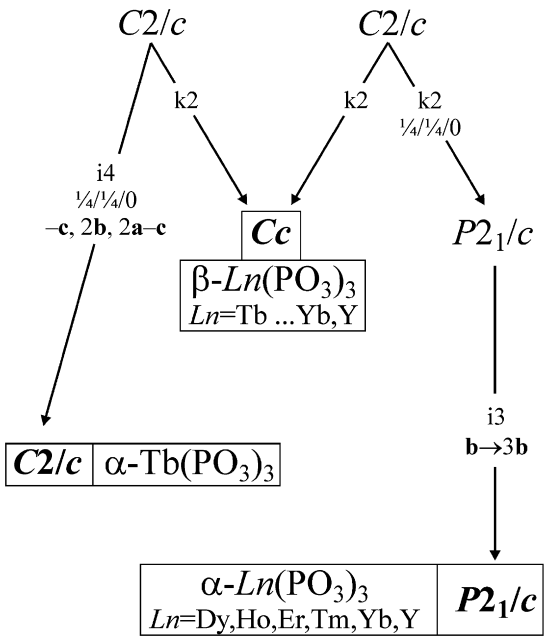

Fig. 5. Symmetry relations between the space groups of the basic unit cell of β-$Ln(PO_3)_3$ (Ln = Y, Tb ... Yb) and the lock-in phases α-$Tb(PO_3)_3$ and α-$Ln(PO_3)_3$ (Ln = Y, Tb ... Yb).

4.4. $Sc(PO_3)_3$

$Sc(PO_3)_3$ is isotypic with $Lu(PO_3)_3$ [8] and *C*-type phosphates like $Al(PO_3)_3$ [19] or $Cr(PO_3)_3$ [20]. The structure model was refined as a threefold superstructure of the basic unit cell in space group *Cc* (Fig. 3). In contrast to the above-mentioned lock-in phases α-$Ln(PO_3)_3$ (Ln = Dy, Ho, Er, Tm, Yb, Y) the crystal structure of $Sc(PO_3)_3$ conserves the *C*-centring which can be clearly seen from Fig. 3.

In $Sc(PO_3)_3$ the Sc atoms are coordinated sixfold in an almost octahedral arrangement with Sc–O distances between 204 and 211 pm. The distances between bridging oxygen atoms and P lie between 155 and 162 pm, and for terminal oxygen atoms distances in the range from 144 to 150 pm to adjacent P atoms are found. All these bond lengths are in accordance with the sum of ionic radii of the respective ions [16]. I can thus confirm the crystal structure determination of [21].

5. Deviation of the phosphate tetrahedra from ideal symmetry

The unacceptably high distortion of some phosphate tetrahedra from the ideal symmetry found in *catena*-phosphates mentioned in the Introduction will be determined and compared with the crystal structure elucidations presented in [8,3] and this contribution.

The deviation from ideal symmetry was calculated applying the method of all ligands enclosing spheres on experimental data. In this method not only distance variations inside a polyhedron are considered but also angle deviations caused by larger distortions. In a first step the optimum centroid of the four surrounding oxygen atoms, i.e. the phosphorus atom is determined by a least-squares refinement [12] and gives a medium centroid-ligand distance r_{centr}. Subsequently, the volume of an ideal tetrahedron given by

$$\frac{8r_{centr}^3}{9\sqrt{3}} \tag{2}$$

is calculated using r_{centr}. Finally this volume is compared with the volume of the experimentally obtained body built up by four vertices [13]. This volume can be calculated using

$$\frac{S \cdot h}{3} \tag{3}$$

where S is the base area built from three vertices and h is the height of the body obtained by the distance from the fourth vertex from the base. The calculated deviations of the found phosphate tetrahedra are presented in Table 5 and amount in very good refined crystal structures like $Sc(PO_3)_3$ to values well below 1.0%. Of course, the PO_4 tetrahedra in *catena*-phosphates will never adopt the shape of an ideal tetrahedron due to partial P–O double-bond contributions to terminal oxygen atoms. From Table 5 it can be clearly seen that the deviations of the corrected structure models show significantly better values than published before. It is thus possible to quantify the otherwise only by eye observable strange distortions. The relatively larger deviations for the incommensurately modulated structures can be assigned to distance variations.

Table 5
Relative deviations of PO_4 tetrahedra; given are the optimised P–O distance (r_{centr}) and the relative deviation of the experimentally obtained tetrahedron from an ideal tetrahedron with r_{centr}.

	$Sc(PO_3)_3$ (this work)	β-$Y(PO_3)_3$ (this work)	$Yb(PO_3)_3$ [3]	α-$Yb(PO_3)_3$ (this work)	β-$Dy(PO_3)_3$ [8]
No. tetrahedra	9	3	9	9	3
r_{centr} (Å)	1.514–1.534	1.482–1.502	1.478–1.545	1.523–1.538	1.461–1.540
Deviation (%)	0.14–0.41	0.51–3.45	0.49–6.89	0.23–0.57	0.66–3.23

Acknowledgments

I would like to thank Prof. Dr. H. Hillebrecht, Albert-Ludwigs-Universität Freiburg, for valuable discussions and generous support. I also thank Mrs. A. Becherer, Albert-Ludwigs-Universität Freiburg, for measuring the vibrational spectra. Financial support by the Fonds der Chemischen Industrie (Liebig Habilitationsstipendium) is gratefully acknowledged.

Appendix A. Supplementary materials

Supplementary data associated with this article can be found in the online version at doi:10.1016/j.jssc.2009.02.036.

References

[1] T. Jüstel, H. Nikol, C. Ronda, New developments in the field of luminescent materials for lighting and displays, Angew. Chem. Int. Ed. Engl. 37 (1998) 3084.
[2] H.A. Höppe, Recent developments in the field of inorganic phosphors, Angew. Chem. Int. Ed. Engl. 48 (2009) 3572–3582.
[3] H.Y.-P. Hong, The crystal structure of ytterbium metaphosphate, YbP_3O_9, Acta Crystallogr. B 30 (1974) 1857–1861.
[4] G.I. Dorokhova, O.G. Karpov, The crystal structure of a new modification of TrP_3O_9(Tr = Er), Kristallografiya 29 (1984) 677–680.
[5] A. Durif, Crystal Chemistry of Condensed Phosphates, Plenum Press, New York, 1995.
[6] C. Ronda, Luminescent materials with quantum efficiency larger than 1, status and prospects, J. Lumin. 100 (2002) 301–305.
[7] A. Shalav, B.S. Richards, T. Trupke, K.W. Krämer, H.U. Güdel, Application of $NaYF_4 : Er^{3+}$ up-converting phosphors for enhanced near-infrared silicon solar cell response, Appl. Phys. Lett. 86 (2005) 13505.
[8] H.A. Höppe, S.J. Sedlmaier, The crystal structure of incommensurately modulated $Ln(PO_3)_3$(Ln = Tb…Yb) and commensurate $Gd(PO_3)_3$ and $Lu(PO_3)_3$, Inorg. Chem. 46 (2007) 3467–3474.
[9] E.V. Murashova, N.N. Chudinova, A.B. Ilyukhin, Erbium tris(trioxophosphate(v)), Crystallogr. Rep. 52 (2007) 230–234.
[10] H.A. Höppe, The synthesis, crystal structure and vibrational spectra of α-$Sr(PO_3)_2$ containing an unusual catena-polyphosphate helix, Solid State Sci. 7 (2005) 1209–1215.
[11] H.A. Höppe, Synthesis, crystal structure and vibrational spectra of $Ca_4P_6O_{19}$ (Trömelite)—a catena-hexaphosphate, Z. Anorg. Allg. Chem. 631 (2005) 1272–1276.
[12] T. Balic-Žunic, E. Makovicky, Determination of the centroid or 'the best centre' of a coordination polyhedron, Acta Crystallogr. B 52 (1996) 78–81.
[13] E. Makovicky, T. Balic-Žunic, New measure of distortion for coordination polyhedra, Acta Crystallogr. B 54 (1998) 766–773.
[14] M. Siemens Analytical X-ray Instruments Inc., Shelxtl X-ray single crystal analysis system, version 5.1.
[15] V. Petricek, M. Dusek, L. Palatinus, Structure Determination Software, Institute of Physics, Praha, Czech Republic, 2006.
[16] R.D. Shannon, C.T. Prewitt, Effective ionic radii in oxides and fluorides, Acta Crystallogr. B 25 (1969) 925–946.
[17] S. Andersson, On the description of complex inorganic crystal structures, Angew. Chem. Int. Ed. Engl. 22 (1983) 69–81.
[18] H.A. Höppe, G. Kotzyba, R. Pöttgen, W. Schnick, High-temperature synthesis, crystal structure, optical properties, and magnetism of the carbidonitridosilicates $Ho_2[Si_4N_6C]$ and $Tb_2[Si_4N_6C]$, J. Mater. Chem. 11 (2001) 3300–3306.
[19] H. van der Meer, The crystal structure of a monoclinic form of aluminium metaphosphate, $Al(PO_3)_3$, Acta Crystallogr. B 32 (1976) 2423–2426.
[20] M. Gruss, R. Glaum, Refinement of the superstructure of C-type chromium(iii) tris(metaphosphate), $Cr(PO_3)_3$, Acta Crystallogr. C 52 (1996) 2647–2650.
[21] A.I. Domanskii, Y.F. Shepelev, Y.I. Smolin, B.N. Litvin, Crystal structure of the low-temperature form of scandium metaphosphate $Sc(PO_3)_3$, Kristallografiya 27 (1982) 229–232.